**Iraqi National Journal of Earth Science**

**www.earth.mosuljournals.com**

# Porosity Type Determination Using the Velocity Deviation Technique for The Sheikh Allas Formation in The Kirkuk Oil Field, Northeastern Iraq

**Dhuha M. Ebrahim [1*], Maan H. Al-Majid [2], Rafee E. Al-Hamidi [3], Saad A. AL Hamdani [4]**

*[1,3] Department of Geology, College of Science, University of Mosul, Mosul, Iraq.*
*[2] Department of Petroleum Reservoir Engineering, College of Petroleum and Mining Engineering, University of Mosul, Iraq.*
*[4] North Oil Company, Ministry of Oil, Iraq.*

**Article information**

**Received:** 19- Feb -2023

**Revised:** 27- Mar -2023

**Accepted:** 09- Apr -2023

**Available online:** 31- Dec – 2023

**Keywords**:
Porosity
Velocity deviation
dolomitization
Sheikh Allas Formation
Kirkuk oil field

**Correspondence**:
**Name:** Dhuha M. Ebrahim

Email: dumahmood@gmail.com

## ABSTRACT

The current study aimed to show the utility of the velocity deviation technique in determining the porosity types of Sheikh Allas Formation in the Kirkuk oil field. Log data collected from two wells in the study area (k-218, and k-246) were analyzed. 46 thin section slides performed by different cutting samples at certain depths were used to identify porosity types. The sonic log was utilized to estimate the true velocity, while neutron and density logs were employed to estimate porosity. Velocity deviation was calculated by subtracting the porosity log velocity from the sonic log velocity. The results revealed that there is a significant agreement in the directions of increase and decrease between the secondary porosity produced by the dolomitization and the velocity deviation. The amount of dolomite in well k-218 increased significantly, as indicated by the higher neutron porosity than density porosity. The high agreement between the neutron porosity and density porosity in well k-246 indicates that the dolomitization process has little effect in this well. By observing the velocity deviation curves, it was found that there is a clear difference between the two wells in the types and depths of the porosities. The secondary porosity in well k-246 does not exceed 5%, while it reaches 15% at some depths in well k-218. It is the most obvious difference between the two wells, resulting from the increase in the percentage of dolomite in well k-218, which may indicate the proximity of well k-218 to the coastal environment. Furthermore, the abnormally high primary porosity that appears at various depths in well k-218 is a feature of this well. A high consistency between the thin section information and the velocity deviation technique in terms of porosity types and their locations was observed. Resistivity logs are also used in this study to identify the permeability locations.

DOI: 10.33899/earth.2023.139106.1059, 

# استخدام تقنية انحراف السرعة في تحديد انواع المسامية لتكوين شيخ علاس في حقل كركوك النفطي، شمال شرقي العراق

ضحى محمود ابراهيم [1*] ، معن حسن الماجد[2] ، رافع إبراهيم الحميدي[3] ، سعد احمد محمود الحمداني [4]

[3،1] قسم الجيولوجيا، كلية العلوم، جامعة الموصل، الموصل، العراق.
[2] قسم هندسة المكامن النفطية، كلية هندسة النفط والتعدين، جامعة الموصل، العراق.
[4] شركة نفط الشمال، وزارة النفط ، العراق.

**معلومات الارشفة**

**تاريخ الاستلام:** 19- فبراير -2023

**تاريخ المراجعة:** 27- مارس -2023

**تاريخ القبـول:** 09- ابريل -2023

**تاريخ النشر الالكتروني:** 31- ديسمبر -2023

**الكلمات المفتاحية:**
المسامية
تقنية انحراف السرعة
الدلمتة
تكوين شيخ علاس
حقل كركوك النفطي

**المراسلة:**
**الاسم:** ضحى محمود ابراهيم
Email:dumahmood@gmail.com

**الملخص**

تهدف الدراسة الحالية الى استخدام تقنية انحراف السرعة في تحديد أنواع المسامية لتكوين شيخ علاس في حقل كركوك النفطي. تم تحليل بيانات الجس البئري لبئرين مختارين في منطقة الدراسة من أجل الحصول على معلومات المسامية ومقارنتها مع بيانات 46 شريحة مقطعية رقيقة مأخوذة من نفس البئرين. تم توظيف بيانات المجس الصوتي في ايجاد السرعة الحقيقية, في حين استخدمت بيانات مجسي الكثافة والنيوترون في حساب المسامية ومن ثم تحويلها الى سرع. مقدار انحراف السرعة موضوع البحث يساوي حاصل طرح السرعة المستنتجة من المسامية من السرعة الحقيقية المحسوبة من المجس الصوتي. أثبتت الدراسة أن هناك توافق كبير في اتجاهات الزيادة والنقصان لكل من انحراف السرعة والمسامية الثانوية في كلا البئرين. لوحظ من بيانات الجس البئري وجود زيادة واضحة في عملية الدلمتة في البئر الأول k-218 مقارنة مع البئر الثاني k-246 والذي قد يعزى الى قرب الأول من البيئة الساحلية وفيرة المياه. من خلال ملاحظة قيم المسامية الثانوية التي تجاوزت 15% في البئر الأول ولم تتجاوز 5% في البئر الثاني يتضح أن معظم المسامية الثانوية قد تكون ناتجة عن عملية الدلمتة مع نسبة قليلة من الكسور والفواصل. علاوة على ذلك, تميز البئر الأول بوجود قيم عالية غير طبيعية للمسامية الأولية عند بعض الأعماق ما قد يشير الى وجود أنطقة كسور أو ربما زيادة في حجم السجيل في تلك الأعماق. وأخيرا لوحظ بما لايقبل الشك وجود توافق كبير بين معلومات المسامية المأخوذة من الشرائح المقطعية الرقيقة مع تلك المستنتجة من تقنية انحراف السرعة للعديد من الأعماق.

DOI: 10.33899/earth.2023.139106.1059, 

## Introduction

A complete analysis of petrophysical properties is essential for comprehending the factors influencing the quality of the petroleum reservoir and the quantity of its productivity (Al-Baldawi, 2021). The primary tool for describing petrophysical properties such as lithology, porosity, and permeability is the well log (Albeyati et al., 2021). The petrophysical characteristics of carbonate rocks in various Iraqi oil reservoirs have been investigated by numerous researchers (Al-Majid, 2019, 2021, 2022; Abdulrahman et al., 2018; Al-Jaberi and Al–Mayyahi, 2018; Al-Jawad and Kareem, 2016; Mamaseni, 2020; Al-juraisy, and Al-Majid, 2021).

The porosity is one of the most important petrophysical characteristic to determine the petroleum volume and the basis for deciding whether a specific petroleum region is economical or not. For carbonate drill hole measurements, sonic, density, and neutron-porosity logs have been routinely used (Al-Majid, 2021).

The velocity deviation technique is one of the important well logging methods used to identify different types of porosity and track permeability trends within rocks (Al-Baldawi, 2020). It is performed using the neutron log or density log along with the sonic log. This technique can be utilized to monitor diagenetic process distribution and to evaluate permeability trends. The log of velocity deviation is created by finding the variance between the true borehole velocity (derived from the sonic log) and the velocity deduced from the neutron log or density log.

The current study aims to delineate the petrophysical properties of early Oligocene Sheikh Allas Formation using well log data. The velocity deviation technique is used to enhance the outcomes of a sedimentary evaluation of (46) thin section slides for two selected wells (K-218, and K-246) in the study area.

## Site Description

Kirkuk oil field is one of the most super giant carbonate oil field in Iraq. It is located about (3.5 km) northwest of Kirkuk City. It extends in about 100 km length and 4.5 km width (Fig.1).


**Fig.1. A site map showing the locations of the two studied wells (modified by the United Nations, 2014).**

The current study area is tectonically located in the northeastern part of Iraq within the unstable shelf in the foothill zone. This zone is characterized by the presence of convex, longitudinal, narrow and asymmetrical folds separated from each other by wide depressions (syncline folds). It is also characterized by a thick sedimentary cover (Jassim and Goff, 2006).

The Kirkuk oil field consists of three main domes. The northern one (Khurmala) is considered as a gas dome. While the middle dome (Avana) contains layers suitable as an oil reservoir. The third dome (Baba) representing the study area is located in the southeast part of the field within the Kirkuk zone with a reverse fault (Kirkuk fault) passes through it. (Jassim and Goff, 2006). Figure (2) shows the structural map of the study area.

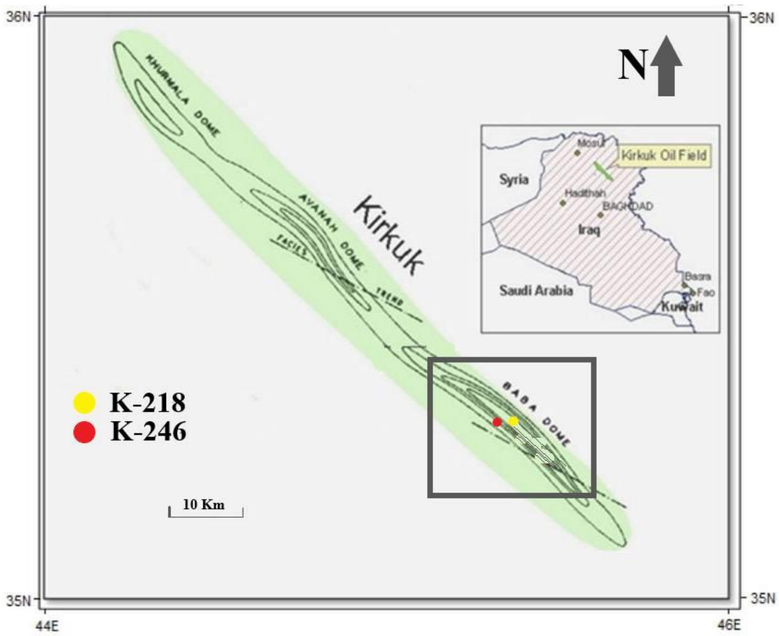


**Fig. 2. A structural map of the study area showing the location of the two studied wells (Majid & Veizer, 1986)**

Stratigraphically, Sheikh Allas carbonate Formation is the earliest Oligocene reefs and forereefs. It has high porosity and permeability, which makes it an important reservoir in the Kirkuk oil field (Aljwaini, 2015). This formation has been described in both sedimentary and stratigraphic terms by many researchers (Bellen, 1956; Kharajiany, 2008; Ghafor, 2011; Al Banna et al., 2013; ALjwaini, 2015; Hawaf, 2022 and Albayati, 2023)

Sheikh Allas Formation consists of porous rubbly dolomitic and recrystallized limestone. The thickness of this formation in the study area is more than 30 m (Table 1).

**Table 1: The depth and thickness of Sheikh Allas Formation in the two studied wells**

| Wells | Formation | Top of formation | Bottom of Formation | Thickness(m) | Location(UTM) |
|---|---|---|---|---|---|
| K218 | Sheikh Allas | 509 | 540 | 31 | E:437457,000<br>N:3933913,0 |
| K246 | Sheikh Allas | 468 | 510 | 42 | E:438959,082<br>N:3933909,3 |

The formation is conformable with its upper contact (Shurau Formation) and with its lower contact (Palany Formation) (Jassim and Goff, 2006). Figure (3) shows the stratigraphic column of Sheikh Allas Formation for both studied wells

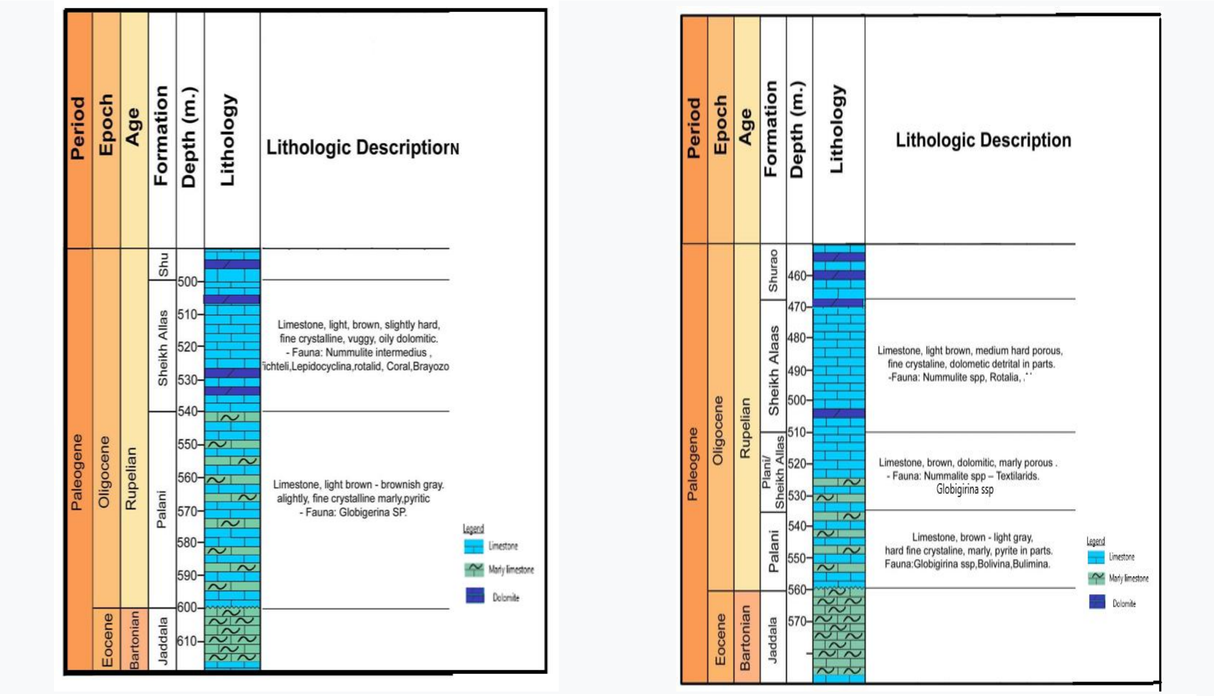


**Fig.3. The stratigraphic column of Sheikh Allas Formation, according to the final report of the Iraqi north oil company, wells (k-246, and K-218)**

## Materials and Methods

In this study, the available logging data for two selected wells ( K-218, and K-246) were used. They are; Gamma ray (GR), Neutron (NPHI), Density (RHOB), Sonic (DT), and resistivity logs (Deep laterolog (LLD), Shallow laterolog (LLS), Micro spherical log (MSFL)). Nuralog (NL), and Interactive Petrophysics (IP V3.5) programs have been utilized to obtain the necessary results and interpret them.

### 1. Formation Evaluation

### 1.1. Porosity

The most crucial feature of reservoir rocks, as it relates to the diagenetic process and burial depth, is porosity. There are two types of porosity: primary, which forms concurrently with deposition, and secondary, which arises during diagenesis (Flugel, 2004). Following the classification of porosity given by Choquette and Pray (1970 ) (Fig. 4), there are numerous forms of porosity that can be recognized within this study.

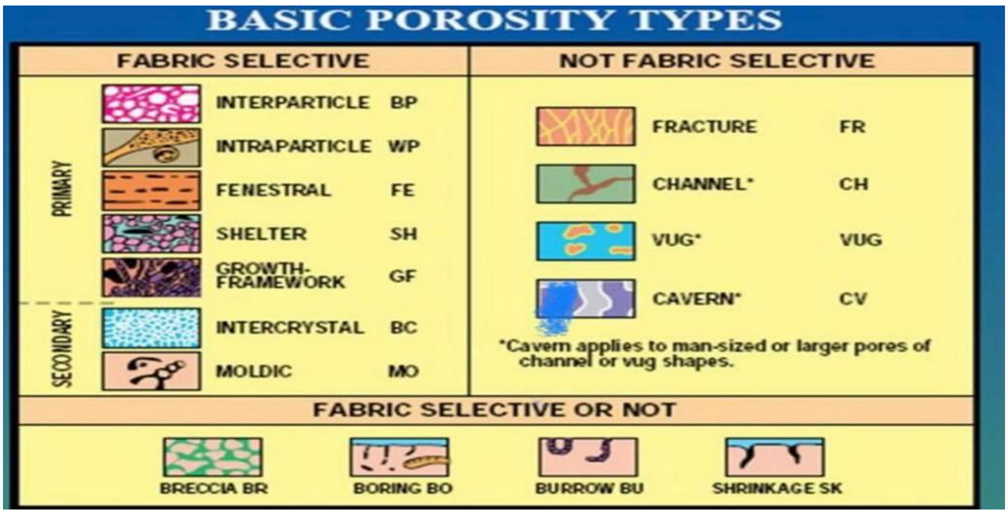


**Fig. 4. Basic porosity types (Choquette and pray, 1970)**

### 1.1.1 Fabric selective pores

**A. Interparticle Porosity**

This primary porosity, which formed between particles in the fabric, is a fabric-specific pore.

**B. Intraparticle porosity**

It is a type of pore space that occurs within grains and is either of primary origin or formed as a result of organic material deterioration in calcareous skeletons (Lonoy, 2006). It is identified at a depth of 530 m in well K218 (Fig. 5).

**C. Intercrystalline porosity**

It was described by Lonoy (2006) as porosity between crystals that had either a primary or secondary porosity. Secondary porosity (inter-crystalline pores) is caused by dolomitization or calcite recrystallization (Heide, 2008). This type of porosity is found at a depth of 526 m in well K218 (Fig. 5) and 483m in well k-246 (Fig. 6).

**D. Moldic porosity**

They are mainly generated through dissolution, and either depositional conditions or diagenetic processes control their distribution (Heide, 2008). According to Flugel (2004), this type of porosity develops in meteoric-phreatic environments, which is noted at the lower part of formation (from 490 m to 510 m) in well K246 (Fig. 6).

**1.1.2. Non-fabric selective pores**

**A. Fracture and Channel porosities**

Fracture is created during the burial diagenetic processes that occur during syn-deposition, deposition, or post-deposition. As a result of promoting overload before cementation, faulting, folding, and fluid over pressure, the rocks breaking is primarily caused by brittle fracture of shells; while channel porosity is a secondary pore that occurs when the openings are significantly enlarged and has developed independently of texture (fabric). The fracture porosity is found in some parts of the formation at the depths of 515 m and 527 m in well K218(Fig. 5), and 469 m in well K246 (Fig. 6); whereas channel porosity is found in the upper part of the formation at a depth of 515 m in well K218 (Fig. 5), and middle part of the formation at a depth of 495 m in well K246 (Fig.6). .

**B. Vuggy porosity**

This type of porosity is caused by unequally distributed early-late diagenetic dissolution that cuts across cement boundary lines or grains (Flugel, 2004). The vuggy porosity is detected in the two studied wells; it is noted in the well K218 at the depths of 513 m and 526 m (Fig. 5); whereas it is detected in the middle and lower parts of the formation in well K246 (Figs. 6).

**C. Cavern porosity**

Large caverns are the defining feature of this non-fabric selective porosity, which also refers to bigger spaces of channel or vugg shapes that are primarily generated by karstic solution processes. This type of porosity is rarely detected in Sheikh Allas Formation.

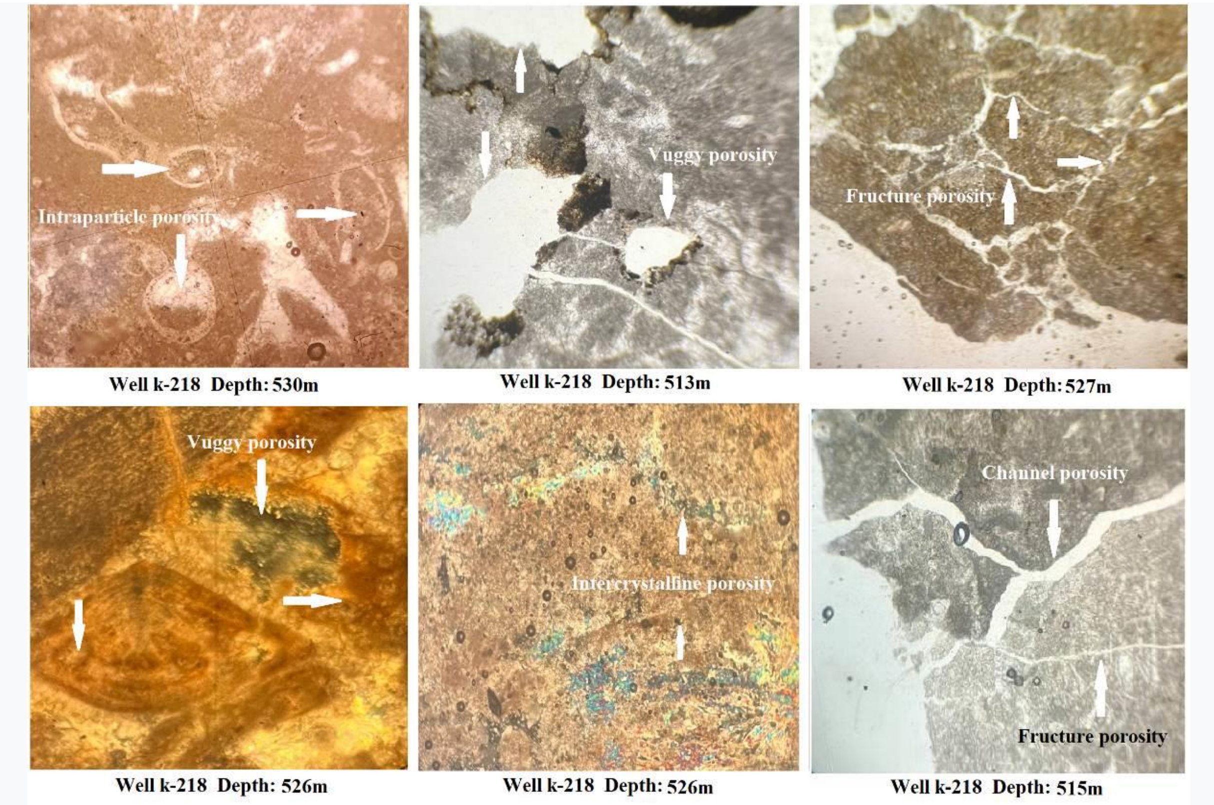


**Fig.5. Photomicrographs of six samples from well k-218 showing the major pore types in Sheikh Allas Formation.**

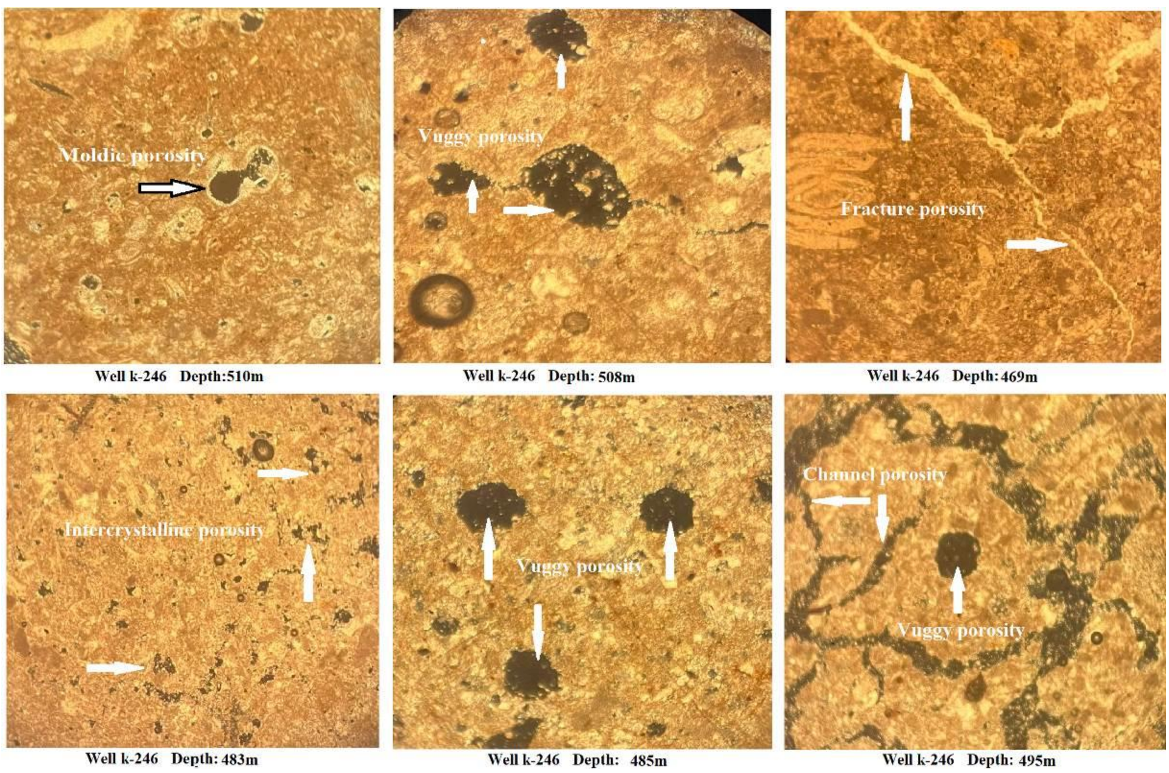


**Fig.6. Photomicrographs of six samples from well k-246 showing the major pore types in Sheikh Allas Formation.**

The main task in this study is to calculate all porosity kinds from neutron, density, and sonic logs using the following equations after completing the appropriate corrections.

$$PHIT = \frac{NPHI + PHID}{2} - - - - - - - - - - - - - - - (1)$$

$$PHID = \frac{\rho ma - \rho log}{\rho ma - \rho f} - - - - - - - - - - - - - - - - (2)$$

$$PHIS = \frac{\Delta tlog - \Delta tma}{\Delta tf - \Delta tma} - - - - - - - - - - - - - - - (3)$$

$$PHIsec = PHIT - PHIS \quad - - - - - - - - - - - - - - (4)$$

Where (Δtf) is the transit time fluid in µsec/ft (189 µsec/ft for water), (Δt) is the reading of sonic log in µsec/ft, (Δtma) is the transit time of matrix in µsec/ft ( 47.5 µsec/ft for limestone), (ρma) is the density of matrix (2.71 g/cc for limestone), (ρf) is the density of fluid (1 g/cc for freshwater), (ρlog) is the reading of density log in g/cc, NPHI is the neutron porosity (the reading of neutron log), PHID is the density porosity (derived from density log), PHIS is the primary porosity (deduced from the sonic log), PHIT is the neutron - density porosity, and PHIsec is the secondary porosity (Boddy and Smith, 2009).

Before starting the interpretation procedure, various adjustments (casing weight, tool diameter, mud weight) for well data reading are performed since certain conditions might have an influence on this data. Making the appropriate modifications to the porosity values derived from porosity logs requires the calculation of shale volume, as in the following equations:

$$Vsh = 0.33 \times \left[2^{(2 \times IGR)} - 1\right] - - - - - - - - - - - (5)$$

$$IGR = \frac{GRlog - GRmin}{GRmax - GRmin} - - - - - - - - - - - - - - (6)$$

$$PHISc = PHIS - (Vsh \times PHISsh) - - - - - - - - (7)$$

$$NPHIc = NPHI - (Vsh \times NPHIsh) - - - - - - - (8)$$

$$PHIDc = PHID - (Vsh \times PHIDsh) - - - - - - - (9)$$

$$PHIE = \text{I} \quad \mathbf{PHI} \quad (1 - Vsh) - - - - - - - - - (10)$$

where GRlog is the gamma ray reading from the GR log, GRmax is the highest gamma ray reading recorded in the well log, and GRmin is the lowest gamma ray reading recorded in the well, PHIDc, PHISc, and NPHIc are the corrected Density, Sonic, and Neutron porosity respectively. PHIDsh, PHISsh, and NPHIsh are Density, Sonic, and Neutron porosity of shale respectively.

**1.2. Lithology**

Sonic, density, and neutron logs should be coupled to identify the lithology information (Dawei et al., 2016). As a result, two diagrams must be instructed: the first is the cross plot of RHOB / NPHI, and the second is the cross plot of M-N.

Where, M, and N factors can be calculated using equations (11, and 12 respectively),

$$M = \left(\frac{\Delta tf - \Delta tlog}{\rho b - \rho f}\right) * 0.01 - - - - - - - - - - - - - (11)$$

$$N = \frac{1 - NPHIc}{\rho b - \rho f} - - - - - - - - - - - - - - - - - (12)$$

(ρb: is the density log reading (ρlog)).

## 2. Velocity Deviation Log

By merging the true velocity log (derived from the sonic log) and the velocity log generated using the equation of time-average (equation 13)(Wyllie et al., 1956), the velocity deviation log has been created as below:

$$\frac{1}{Vrock} = [(1 - \emptyset)/(Vm] + [\emptyset/Vf] ----------(13)$$

Where: Vrock is the required velocity, ϕ is the corrected density porosity (PHIDc), or the corrected neutron porosity (NPHIc) Vm is the matrix velocity (6530 m/s for limestone), and Vf is the fluid velocity (1500 m/s for water), (Flavio and Gregor, 1999).

The velocity deviation (VD) was produced as below:

$$VD = Vsonic - Vneutron \text{ or } Vdensity --------(14)$$

Where: $V_{neutron}$, $V_{sonic}$, $V_{density}$ are the velocities derived from neutron, sonic, and density logs respectively. Sonic velocity is determined from the sonic log after converting the temporal data into velocity,

As a result, the velocity deviation log is employed to determine the permeability pathways and the impact of the various kinds of porosity. In general, the positive velocity deviations are associated with a rise in porosity, which usually causes a rise in permeability, except if unconnected micro porosity is occupied, which in that case permeability decreases (Flavio and Gregor, 1999).

The positive velocity deviations (greater than 500 m/s) reflect zones where velocity is greater than expected based on porosity values, such as zones occupied by frame-forming pore forms. Zero deviations (-500 to 500 m/s) indicate intervals when the rock is not supported by a solid frame, such as in carbonates with significant antiparticle porosity or micro porosity. Fractures, a cavernous hole wall, or the presence of substantial amounts of gas are three factors that might result in a large negative deviation in velocity (less than -500 m/s), and these circumstances can typically be detected by continually recording downhole velocity deviation (Flavio and Gregor, 1999).

# Results

## 1. Lithology Identification

According to neutron-density cross plots (Fig. 7), the major matrix in Sheikh Allas Formation is limestone with a significant amount of dolomite. In addition, there is a small amount of clastic minerals in both wells, which increases more in well K-246.

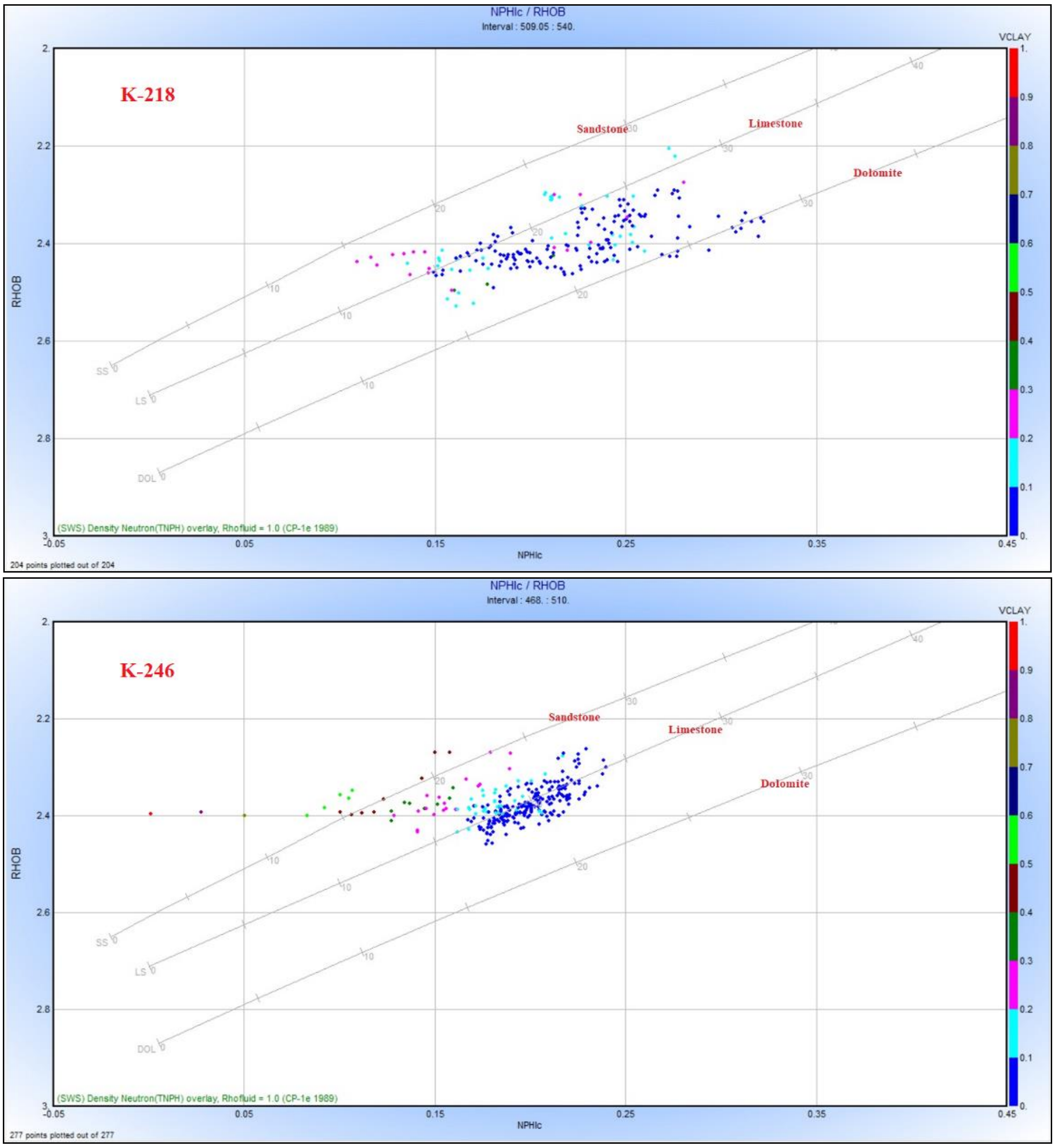


**Fig.7. NPHIc-RHOB cross plots for the two studied wells (K-218, and K-246)**

From figure (7), it is noted that the points gather around the limestone line in well K-246, while they deviate clearly towards the dolomite line in well K-218, which indicates an increase in the percentage of dolomite in this well.

The lithology-dependent parameters M and N allow for the construction of the M-N cross plot, which aids in the identification of the lithology. Figure (8) shows the M-N cross plot for the two studied wells.

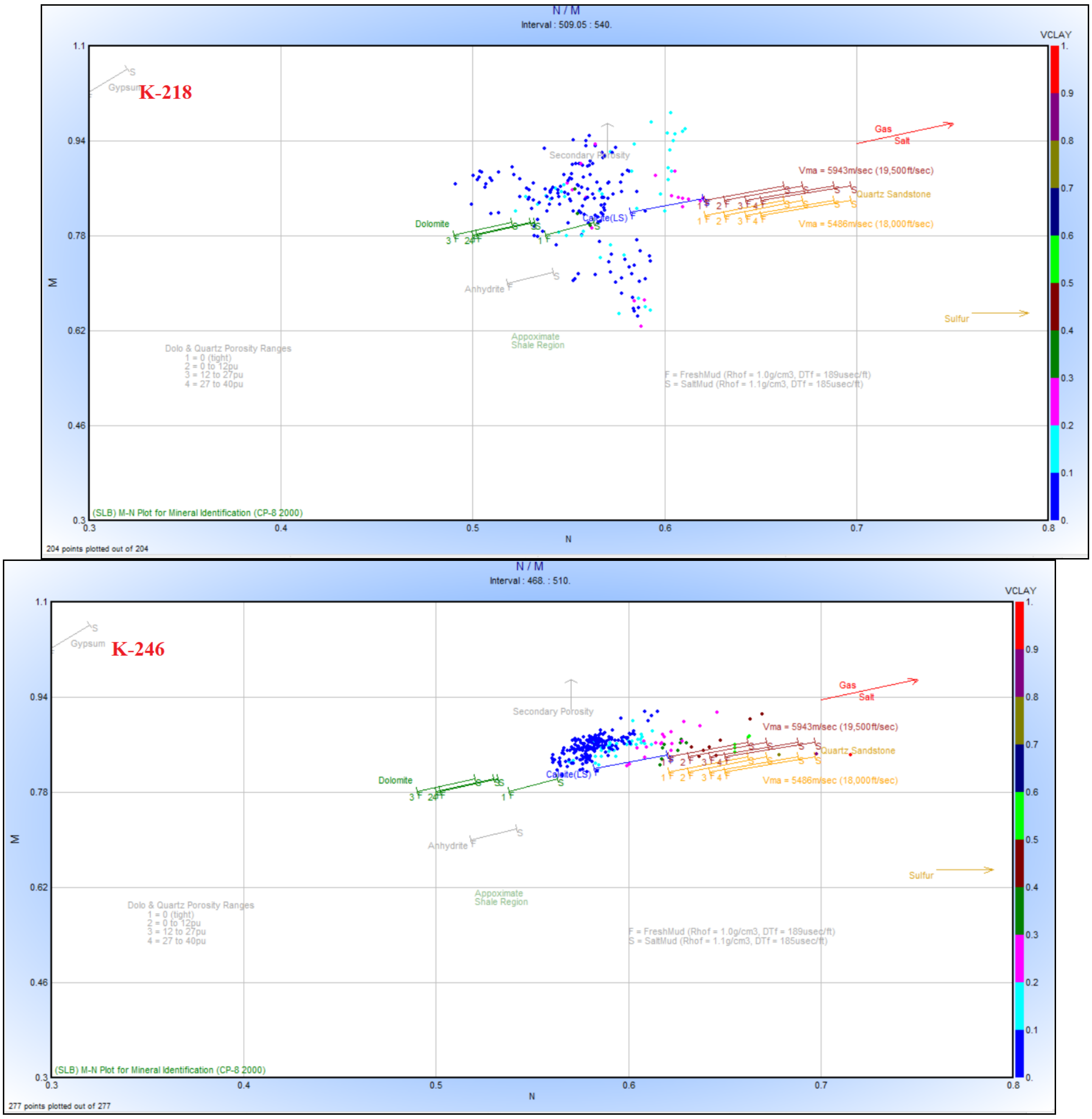


**Fig.8. M-N cross plots for the two studied wells (K-218, and K-246)**

Obviously, the main component of Sheikh Allas Formation is limestone. It is clear that there is a significant increase in dolomite in well K-218 compared to well K-246. The accumulation of points towards the secondary porosity area may be result from an increase of dolomite proportion in this well (Fig. 8).

## 2. Porosity

Porosity values were calculated and plotted after analyzing porosity logs using various software's (Interactive Petrophysics, Neuralog) (Figs. 9, and 10).

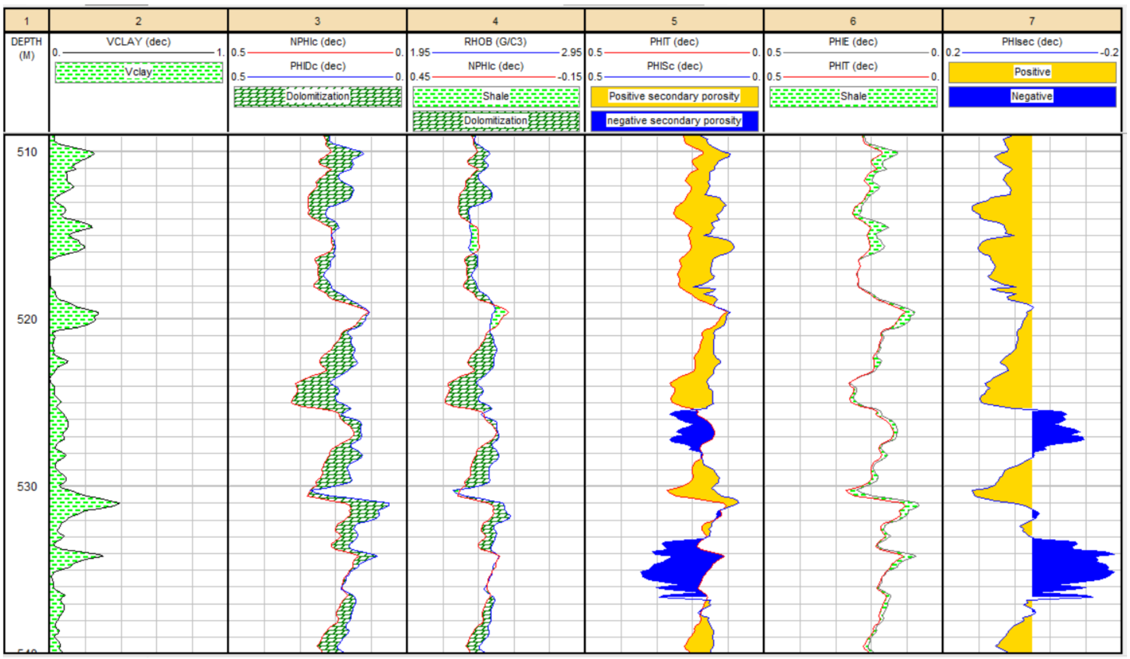


**Fig.9. The all calculated porosity logs showing the dolomitization zones and their relationship with the shale volume in well K-218**

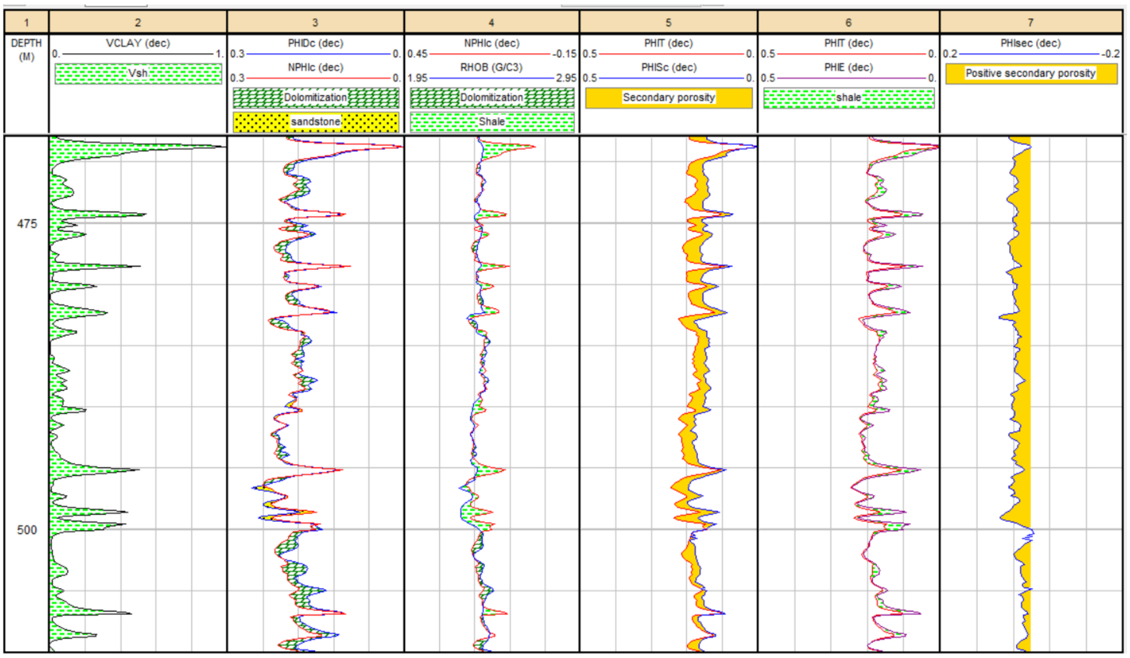


**Fig.10. The all calculated porosity logs showing the dolomitization zones and their relationship with the shale volume in well K-246**

From NPHIc, and PHIDc logs, the dolomitization sites can be distinguished at all depths. An increase in NPHIc with a decrease in PHIDc indicate an increase in dolomite content (shaded by dolomite index). Sheikh Allas Formation has a higher amount of dolomite in well k-218 compared to well k-246 (Figs. 9, and 10). The increase of dolomite in well K-218 is attributed to its proximity to the coast line in comparison with well K-246, the process of dolomitation (mixing zone model), needs a source of magnesium, such ion can be provided by the continent through its meteoric water (Wareen, 2000).

The increase in secondary porosity (PHIsec) in well k-218 confirms the increase in dolomite in this well. PHIsec shows negative values at some depths in well k-218 due to the abnormal increase in the primary porosity (PHISc) relative to the total porosity (PHIT) at those depths. This abnormal increase in PHISc may be derived by fractures or an increase in shale volume. Although there was an increase in shale volume in well k-246, there were no negative values for secondary porosity in this well. Therefore, fractures can be considered as the main cause of negative secondary porosity in the studied formation.

### 3. Velocity deviation

The velocity logs calculated from the sonic, neutron, and density logs are shown in figures (11, and 12). According to the velocity deviation logs ($VD_{density}$ and $VD_{neutron}$), positive deviation zones (gold color) are detected by high porosity and high permeability, except when unconnected microporosity predominates, for such case, the permeability reduces. In intercrystalline, interparticle, or high microporosity zones, deviations of -500 to +500 m/s (light blue color) are common(Flavio and Gregor, 1999). In this study, a big negative deviation in velocity (less than -500 m/s) can be caused by fractures, or a cavernous hole wall.

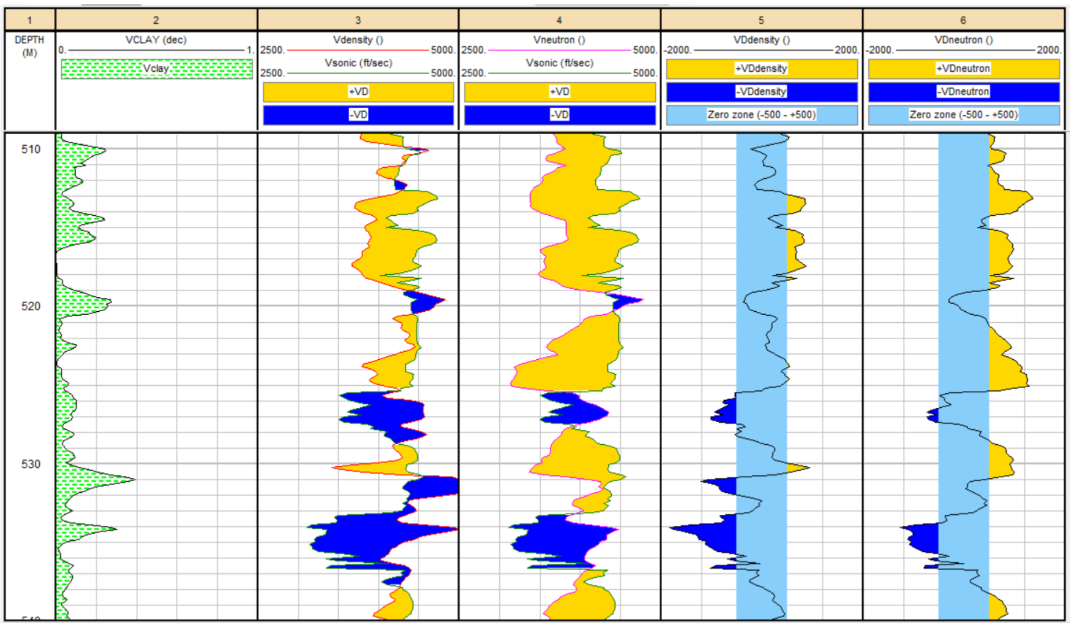


**Fig.11. Velocity deviation logs for well K-218 in the research region display positive zones (gold), negative zones (blue), and zero zones (light blue color) along with the matching Vsh curves.**

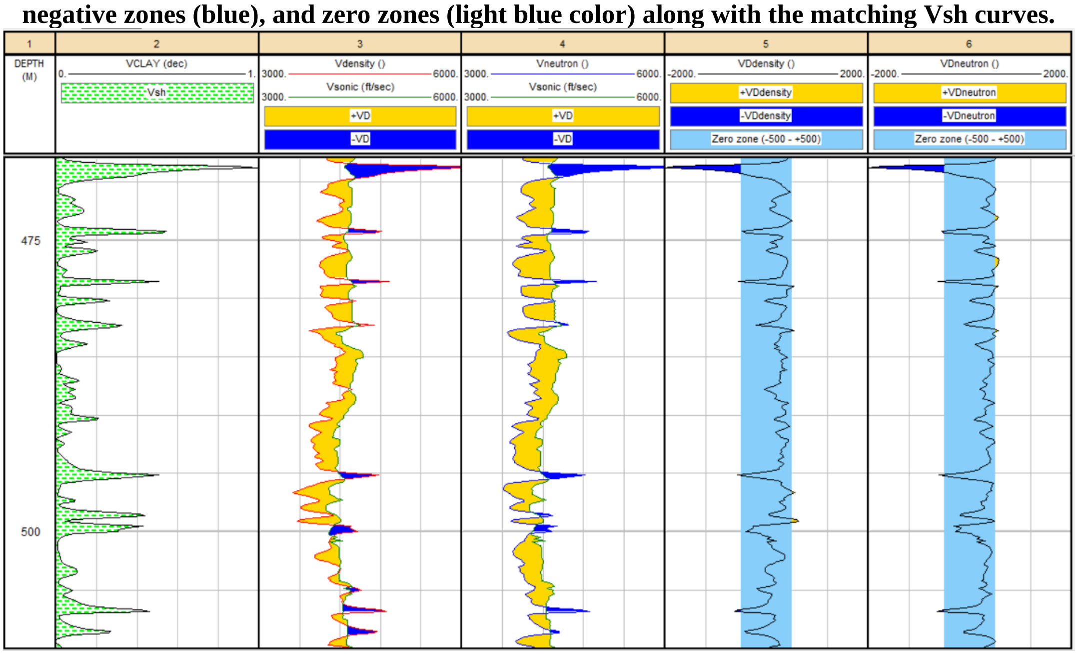


**Fig.12. Velocity deviation logs for well K-246 in the study area display positive zones (gold), negative zones (blue), and zero zones (light blue color) along with the matching Vsh curves.**

# Discussion

To improve the knowledge of the various kinds of porosity and their effect on permeability in the Sheikh Allas Formation, velocity deviation and all porosity logs for the two studied wells are coupled (Figs.13, and 14). In addition, other log data (resistivity, and shale volume logs) are utilized for comparison and explanation.

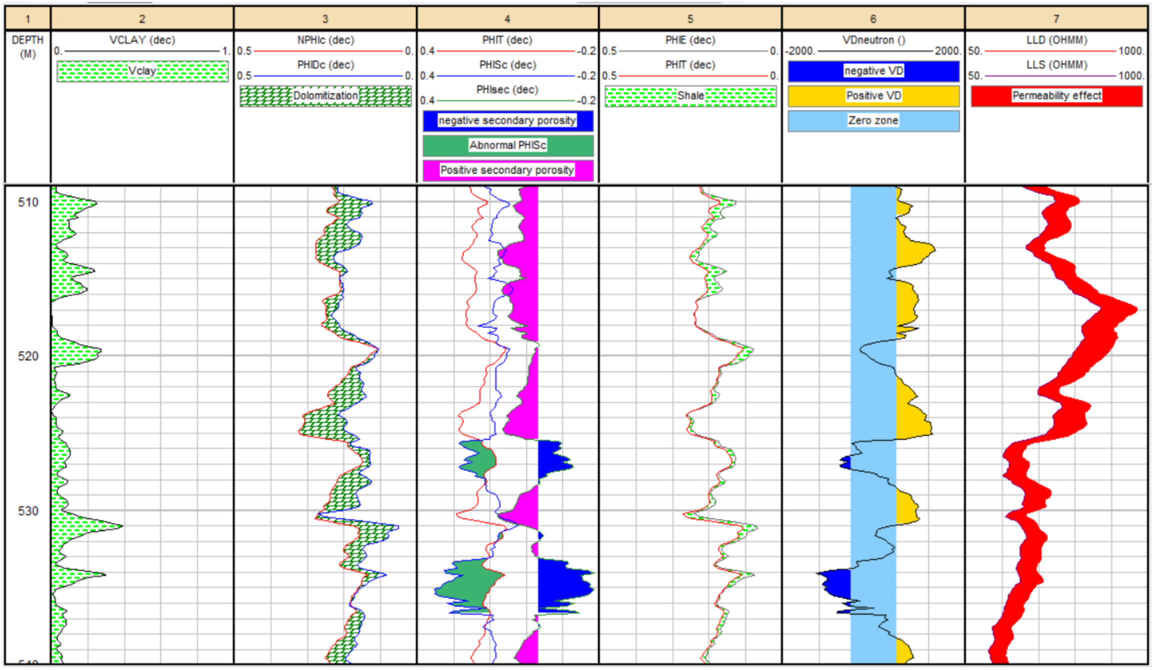


**Fig.13. All logs for well k-218 that are currently available.The gold color symbolizes positive VDneutron curve values( > +500 m/s), light blue reflects VDneutron values ranging from -500 to +500 m/s, dark blue represents negative VDneutron values (<-500 m/s), and red denotes the permeability impact on the two resistivity logs.**

From figure **(**13**)**, PHIsec positive values (track 4) roughly match the positive values of $VD_{neutron}$ (track 6) at all depths. This could imply that this technique is useful for detecting areas with high porosity and permeability. Moreover, unconsolidated (relatively higher shale), or large fracture sites may be inferred from the negative secondary porosity accompanied with the negative velocity deflection. There is a significant decrease in PHIsec values with little shale and little dolomite at interval depths of (525-529 m) and (533-537 m), which could be interpreted as fracture zones intervals. The velocity deviation curve and its relationship with the separation of two resistivity logs (red color) demonstrate that there is still some permeability at most depths. As it is known, the increase in neutron porosity (NPHIc) compared with density porosity (PHIDc) means an increase in the percentage of dolomite .A clear agreement appears between the positivity of secondary porosity and the dolomite sites, which indicates that most types of pores at those depths may have resulted from the dolomitization. The large increase in resistivity values in the upper half of the formation may indicate the presence of hydrocarbons in this part.

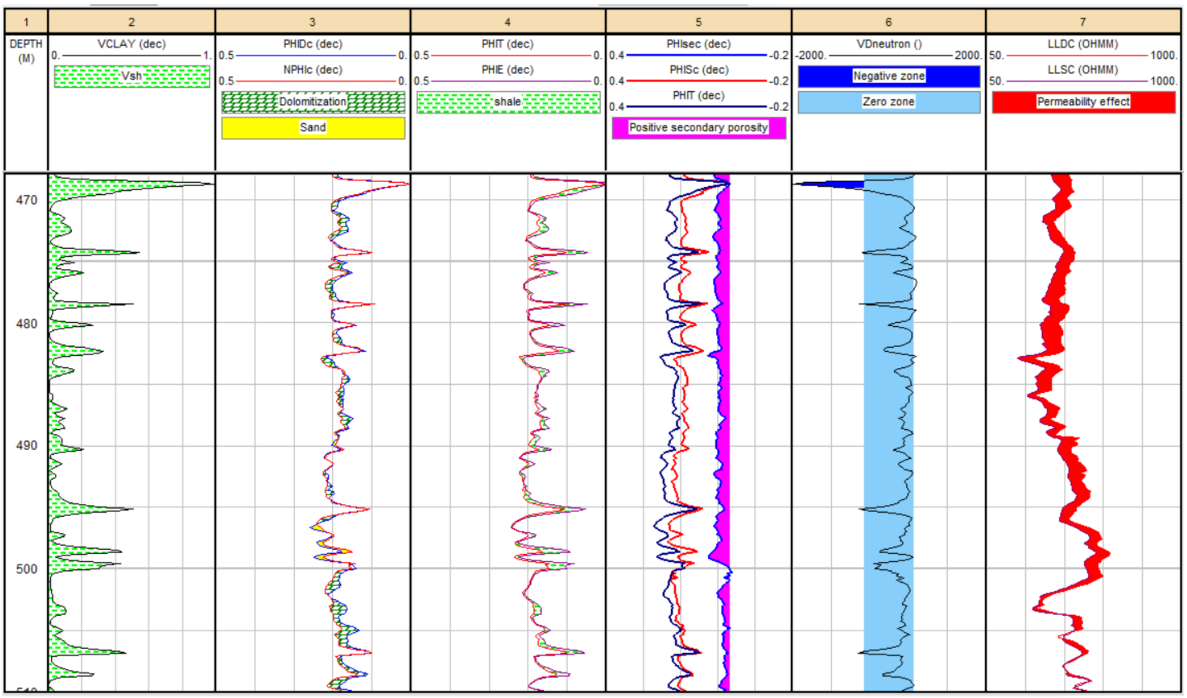

**Fig.14. All available logs for well k-246 . The light blue color reflects $VD_{neutron}$ values ranging from -500 to +500 m/s, red symbolizes the effect of permeability on the resistivity logs, and purple represents positive secondary porosity values.**

From figure 14, **t**he depth 469 m is the only one showing significant negative secondary porosity values, which is the result of the very high value of shale volume at that depth. The secondary porosity of Sheikh Allas Formation in this well is relatively low (maximum 5%) compared to that of well k-268. The great agreement between the values of neutron porosity (NPHIc) and density porosity (PHIDc) in this well indicates that the limestone is l**ess** affected by the dolomitization process at most depths. This may indicate that the dolomitization is the main cause of most of the secondary porosity of the Sheikh Allas Formation in the study area.

$VD_{neutron}$ in the most depths of this well is within the zero zone (-500 to +500), which may indicate intercrystalline, interparticle, or high microporosity zones. An increase in shale volume in this well corresponds to a decrease in resistivity. In addition, the less separation between the resistivity logs compared to well k-268 may indicate a lower permeability of Sheikh Allas Formation in this well. Moreover, the large convergence between the two resistivity curves in the lower part of the formation may indicate a very low permeability in this part.

It is evident by observing the thin section slides at certain depths that there is a good agreement between the types of porosity which are visible in the thin section slides and the porosity inferred from the velocity deviation technique.

## Conclusion

Several conclusions are drawn during this study as follows:

1- Employing the great agreement between the high positivity of each of the velocity deviation and the secondary porosity in the detection of dolomitization sites.

2- Determination of fracture zone locations based on the abnormal values of primary porosity (negative secondary porosity) at the sites of low dolomitization and low shale volume.

3- There is a high level of consistency between the types of porosity deduced by the velocity deviation technique and those seen by the thin sections.

4- The clearly increase of dolomitization coupled with the increase in secondary porosity in well k-218 compared to well k-246 indicates that dolomitization is the main cause of most of the secondary porosity in this study.

## Acknowledgment

The authors would like to express their gratitude to College of Science, College of Petroleum and Mining Engineering at University of Mosul, and the North Oil Company for providing facilities required for this work.

## References

Abdulrahman, S. S., Al-Kubaisi, M. S. and Al-Shara'a, G. H., 2018. Formation evaluation for the Jeribe Formation in the Pika gas field, Iraqi Geological Journal, 53(2F), 83-93 P.

Al Banna, N. Y., Al Mutwali, M. and Ismail, N., 2013. Oligocene Stratigraphy in the Sinjar Basin, northwestern Iraq, GeoArabia, V.15, No.4, PP17-44, Gulf Petro Link, Bahrain.

Al Bayati,Y. K. J., 2023.Sedimentology and sequence stratigraphy of Oligocene succession in selected site of Iraq, ph. .D.(unpublished),university of Tikrit, Iraq 191p.

Al-Baldawi, B. A., 2021. Evaluation of petrophysical properties using well logs of the yammama formation in abu ammod oil field, southern iraq, Iraqi geological journal 54(1e), 67-7 P.DOI: 10.46717/igj.54.1E.6Ms-2021-05-27

Al-Baldawi, B. A., 2020. Determination of pore types and porosity trends using of velocity-deviation log for the carbonate mishrif reservoir in halfaya oil field, southeast Iraq. Iraqi geological journal, 53(1d), pp.26-37. DOI:10.46717/igj.53.1D.3Rw-2020.05.02

Albeyati, F. M. O., Abdula, R.A. and Fikret, T., 2021. Porosity and permeability measurements integration of the Upper Cretaceous in Balad Field, Central Iraq, Iraqi Geological Journal, 54(1B), 24-42.

Al-Jaberi, M. H. and Al -Mayyahi, H. K., 2018. Wireline logging response and true core analysis of the upper shale member of Zubair Formation, Rumaila oilfield, Southern Iraq. Iraqi Geological Journal, pp. 51, 28-40.

Al-Jawad, M. S. and Kareem, K. A., 2016. Geological model of Khasib Reservoir, central area, East Baghdad Field. Iraqi Journal of Chemical and Petroleum Engineering, pp. 17(3), 1-10.https://doi.org/10.31699/IJCPE.2016.3.1

Al-Juraisy, B. A. and Al-Majid, M. H., 2021. Importance of velocity deviation technique and negative secondary porosity in detection of hydrocarbon zones in khasib formation, east Baghdad oil field. The Iraqi geological journal, pp. 86-103.

Al-Jwaini, Y. S. K., 2015. Sequence stratigraphy and reservoir characterization of the late palaeogene - early neogene succession in Kirkuk area” ph. D. Thesis (unpublished), university of baghdad, Iraq 230 p.

Al-Majid, M. H, 2019. New petrophysical equations for Hartha-Tannuma interval in the East Baghdad Oil Field, Iraqi National Journal of Earth Science, 2(19), 136-152.

Al-Majid, M. H., 2021. Petrophysical properties estimation of euphrates reservoir in qayyarah oil field using core and well log data. Iraqi geological journal, 54(2e),pp. 186–197. https://doi.org/10.46717/igj.54.2E.13Ms-2021-11-29

Al-Majid, M. H., 2022. July; The combination of velocity deviation and thorium normalization techniques to detect the Hartha Formation oil zones in the Qayyarah oilfield. In AIP Conference Proceedings (Vol. 2443, No. 1, p. 030001). AIP Publishing LLC. https://doi.org/10.1063/5.0091810

Bellen, R. C. V,1956. The stratigraphy of the main limestone of the kirkuk, bai hassan and qara chauq dagh structures in northern Iraq. Journal of the institute of petroleum, 42, (233- 263).

Boddy, R. and Smith, G., 2009. Statistical Methods in Practice: for Scientists and Technologists. 1st edition Wiley, U.K., 246p.

Choquette, P. W. and Pray, I. C, 1970. Geological nomenclature and classification of porosity sedimentary, A.A.P.G. bulletin, vol. 45 , pp. 207 – 250.

Dawei, C., Xuanjun, Y., Chuanmin, Z., Cong, T. and Mengshi, W., 2016. Logging-lithology identificationmethods and their application: a case study on the chang 7 member in the central-western ordos basin,nw China. China petroleum exploration, pp . 21(5), 1-10.

Flavio, S. A. and Gregor, P. E., 1999. The velocity-deviation log: a tool to predict pore type and permeability trends in carbonate drill holes from sonic and porosity or density logs, AAPG bulletin, pp. 83(3), 450–466.

Flugel, E., 2004. Microfacies of Carbonate Rock, Analysis, Interpretation and Application. Springer-Verlag, Berlin, 976P.

Ghafur, A. A., 2012. Sedimentology and reservoir characteristics of the Oligocene Miocene carbonates (Kirkuk Group) of Southern Kurdistan, Ph.D., pp. (324).

Hawaf., A. H., 2022. Seismic interpretation of shurau and sheikh alas formations in ismail oil field, northern Iraq. Master thesis in geophysics,department of geology,university of baghdad,108p.

Heide, M., 2008. Dispersion and two-phase flow in material from different carbonate pore classes. Master thesis, Petroleum technology–reservoir chemistry, Department of Chemistry University of Bergen. 99p.

Kharajiany, S. O. A. 2008. Sedimentary facies of Oligocene rock units in Ashdagh mountain-Sangaw District-Kurdistan region, NE Iraq, Unpublished M.Sc. thesis, College of Science, University of Sulaymania. pp. (137).

Jassim, S. J. and Goff J. C, 2006; Geology of Iraq , published by dolin , prague and moravian miseum , brno , first edition .pp318.

Lonoy A., 2006. Making Sense of Carbonate Pore Systems: American Association of petroleum Geologists Bulletin, v. 90, no. 9, Pp. (1381-1405).

Majid, A. H. and Veizer, J., 1986. Deposition and chemical diagenesis of Tertiary carbonates Kirkuk oil field, Iraq, AAPG, Bull. ; Vol/Issue:70:6, Univ. of Ottawa, Ontaio. USA .

Mamaseni, W. J., 2020. Petroleum potentiality and petrophysical evaluation of the middle Jurassic Sargelu Formation, Northern Iraq, Iraqi Geological Journal, 53(2D), 77-93.

United Nations, 2014. Iraq administered map, department of field support, cartographic section, map no. 3835 rev. 6.

Wareen, J., 2000; Dolomite. Occurrence, evolution, and economically important association, Earth Science Reviews,Vol.52,PP.1-81.

Wyllie, M. R., Gregory, A. R. and Gardner, G. H. F., 1956. Elastic wave velocities in heterogeneous and porous media. Geophysics, 21(1), 41–70.